1st Latin-American Workshop on Structural Health Monitoring
LATAM-SHM 2023
December, 5-8 2023

# WIND TURBINE CONDITION MONITORING USING AN IMU MOUNTED ON THE HUB

**I. Vilella[†*], G. Gainza[†], M. Zivanovic[*‡], X. Iriarte[※‡], A. Plaza[※], and A. Carlosena[*‡]**

[†] IED Greenpower
Poligono Industrial Plazaola D-14
E-31195, Aizoain, Spain
E-mail : ivilella@iedcompany.com - Web page: https://www.iedcompany.com

[*]Dpt. of Electrical, Electronics, and Communications Engineering
[※]Dpt. of Engineering
[‡]Institute of Smart Cities
Universidad Pública de Navarra (UPNA)
Campus de Arrosadia, E-31006 Pamplona, Spain
E-mail: miro@unavarra.es, https://www.unavarra.es

**Key Words**: Wind Turbines, CMS, IMU, Kalman Filter, Angular Domain.

**Abstract.** *Acceleration sensors for Condition Monitoring in Wind Turbines (WT) are usually placed on non-rotating elements such as the nacelle or the tower. Sensorizing blades, though desirable, is much less frequent since it poses serious practical limitations in terms of powering, communication, installation, and maintenance considering the existing infrastructure.*
*As an alternative to circumvent such limitations we propose the use of an Inertial Measurement Unit (IMU) placed on the rotating hub. This positioning offers two advantages. Firstly, it allows to accurately estimate azimuth in real-time using only one IMU. Secondly, it enhances our sensitivity to the dynamics of the blades and the hub, all while capturing the dynamics of the tower and nacelle.*
*Azimuth is calculated by combining the signals measured by the IMU with a Kalman Filter (KF). This estimation enables three significant capabilities. First, it allows to transform the measured acceleration to a fixed reference frame, as if it were measured in the nacelle or tower. This effectively eliminates the impact of rotation on acceleration signals and demonstrates our improved sensitivity to the blades and rotor, all while continuing to detect nacelle/tower dynamics. Secondly, having the estimated azimuth empowers to detect faults or events associated with rotation. Thirdly, it enables to isolate the analysis of the behaviour of harmonics such as 1P, 3P, 6P, and so on.*
*Validation of this methodology is demonstrated using synthetic signals from OpenFAST, a digital WT modelling and simulation platform.*

## 1. INTRODUCTION

Over time, the wind sector has undergone significant transformations, moving from stringent regulatory requirements on turbine design, validation, and manufacturing to a collaborative environment embracing all key stakeholders, including manufacturers, operators, and maintainers. Central to this collaborative effort is the aspiration to meet the standards outlined in the 61400-28 guidelines, a critical framework that guides the safe and economically viable extension of the operational lifespan of existing turbines.

To fine-tune the estimations regarding the structural health and the remaining useful life (RUL), of wind turbines, a probabilistic approach grounded in real-time measurement and analysis of each turbine's operational data is pivotal. By closely monitoring trends in key indicators, it is possible to tailor the estimation approach more adeptly to actual needs, enhancing both precision and reliability. This methodology accounts for the variability in the dynamic model parameters that structurally represent each turbine and its control system and accommodates the inherent randomness of wind conditions.

In this evolving landscape, Condition Monitoring Systems (CMS) have undergone substantial advancements, evolving from being tools for fault detection and diagnosis in bearings, gears, and other rotary systems to sophisticated systems leveraging the latest in electronic sensing design, data processing, and analytical algorithms [1]. Modern CMS, equipped with advanced alert methods, work in synergy with innovative approaches like the one proposed in this paper, representing a paradigm shift towards a proactive and data-driven approach to monitoring, and thus ensuring safer and more efficient turbine operations [2]. In this context, there is a pressing need for the development of tailored sensor technologies and analytical techniques. These custom solutions should be versatile enough to be applied across various turbine typologies, ensuring robustness and autonomy in both installation and operation. Simplicity in terms of installation is vital, reducing potential barriers to adoption. Additionally, cost-efficiency remains a critical factor, as it directly impacts the feasibility and scalability of these monitoring systems.

In WT operations, the incident wind characteristics and the hub's azimuthal position are critical variables that dictate control strategies. These strategies are designed to act upon the pitch angle of each blade, a crucial aspect that governs the efficiency of wind energy capture by regulating the power absorbed from the wind through control loops focused on torque or rotational speed. The dynamic response of the structure, characterized by sustained deformations, supported loads, and accumulated damage, is a direct outcome of the intricate interplay between operational conditions, control systems, and the turbine's design and manufacturing parameters.

Aligned with sector demands, we propose the use of an IMU placed on the Hub. This strategy aims to enhance sensitivity to hub and blade dynamics while autonomously estimating the necessary information. This is reached without connection to other sensors or devices of the WT, allowing for the separate analysis of the dynamic response of the structure caused by the rotor's rotation effects on one hand, and on the other, the dynamic response of the structure itself at resonance frequencies due to, among other factors, the stochastic excitation of the wind. The IMU incorporates both an accelerometer and a gyroscope, each based on MEMS

technology, which is known for its cost-efficiency. By positioning these sensors on the rotor, we achieve optimal readings with a favorable signal-to-noise ratio, ensuring measurement accuracy. The gyroscope enables precise estimation of the IMU's orientation during its installation. Moreover, the interplay of gravitational acceleration with the hub's rotational movement allows the signal from the accelerometer to determine the rotor's azimuthal position. This facilitates accurate estimation of the turbine's fore-aft oscillation, providing a comprehensive insight into the WT dynamic behavior.

To achieve this, mathematical models representing the fundamental acceleration and angular velocity components of circular motion are incorporated within a Kalman Filter structure. These mathematical models focus on modeling the waveforms from a mathematical perspective rather than relying on dynamic models of the structure [3]. This approach allows for the generalization of the solution to different WT configurations, ensuring broader applicability and versatility. The acceleration data provided by the IMU, combined with the estimation of installation and operational variables, can be projected onto a reference fixed to the ground, effectively eliminating the influence of gravitational acceleration on the frequencies associated with the rotational movement. This data, when analyzed in the frequency domain, can monitor the response related to structural dynamics and its natural frequencies. Additionally, when analyzed in the angular domain in combination with the azimuth, it can be used to diagnose dynamic effects, such as aerodynamic imbalances, associated with the turbine's rotation [4].

## 2. THE METHODOLOGY

The IMU sensor shall be installed in the hub. A defined known radius R is considered, and a generic orientation described by $\beta_1$, $\beta_2$ and $\beta_4$. Besides, two relevant degrees of freedom of the WT are modelled, the hub azimuthal position, described by the angle $\theta$ and the hub tilting corresponding with $\beta_3$. The geometric parameterization used to represent the IMU is shown in Fig 1:

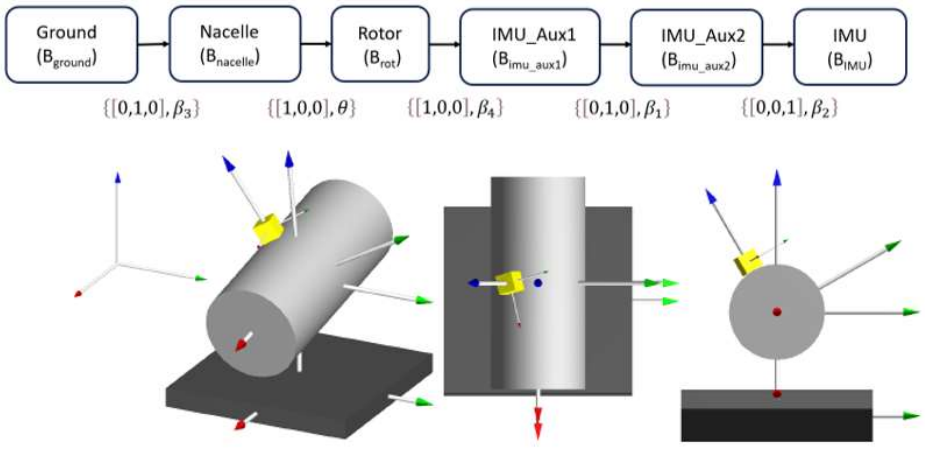


Fig 1. IMU Orientation diagram and reference frames description.

A Kalman Filter structure, which is a recursive filter that estimates the state of a system from a series of noisy or incomplete measurements is going to be used. The KF operates on systems based on two main sources of information, a model used to predict the state in the following step based on the current state estimation, and a measurement related with the state used to update the prediction. Mathematically, the state-transition and measurement equations take the following form:

$$x_{n+1} = f(x_n, u_n) + w_n \quad (1)$$

$$z_n = h(x_n) + v_n \quad (2)$$

Here the vectors $x_n$ and $x_{n+1}$ respectively represent the state of the system at times n and n+1, $z_n$ represents the vector of sensor measurements, and $u_n$ the vector of inputs to the system. The function $\mathbf{f}(\cdot)$ represents the set of functions describing the state-transition model and $\mathbf{h}(\cdot)$ the equations relating the sensor output to the state. Finally, $w_n$ and $v_n$ represent respectively the Gaussian noise vectors, representing the uncertainty on the state-transition and measurement models not coming from uncertainty in the state or input vectors, with zero mean and covariances $\boldsymbol{Q}$ and $\boldsymbol{R}$, respectively.

The strategy for setting up the Kalman Filter will be to define state variables that allow the construction of functions with linear relationships between variables, and at the same time, express mathematically the waveforms recorded by the accelerometer and the gyroscope, whose signals will be used as measurement equations.

Later, the structure of KF will be implemented iteratively, under real time operation context, using just the current measurement values and the previous state estimation. Thus Being $\hat{x}_{n,n}$ and $\hat{P}_{n,n}$ the expected state and covariance matrix estimate at time n given observations up to and including time n, the KF generate the state estimate at time *n+1*:

$$x_n \sim N\left(\hat{x}_{n,n}, \hat{P}_{n,n}\right) \quad (3)$$

$$x_{n+1} \sim N\left(\hat{x}_{n+1,n+1}, \hat{P}_{n+1,n+1}\right) \quad (4)$$

where, $\hat{x}_{n+1,n}$ refers to the estimated expected value of $x$ at sample *n+1* given the observations up to sample *n*. In every iteration the two stages characteristics of the KF are implemented. The first stage of the KF is the so called, prediction stage, where, based on the state-transition equation, the estimated state $\hat{x}_{n+1,n}$ and covariance $\hat{P}_{n+1,n}$ are determined from the previous step estimation, $\hat{x}_{n,n}$ and $\hat{P}_{n,n}$:

$$\hat{x}_{n+1,n} = f(\hat{x}_{n,n}, u) = F_n \hat{x}_{n,n} + G_n u_n \quad (5)$$

$$\hat{P}_{n+1,n} = F_n \hat{P}_{n,n} {F_n}^T + Q \quad (6)$$

The second stage, the so-called correction stage, includes the measurement equation. The estimated values of the state vector $\hat{x}_{n+1,n+1}$ and the covariance matrix $\hat{P}_{n+1,n+1}$ at the following instant are updated with the sensor measurements:

$$\hat{x}_{n+1,n+1} = \hat{x}_{n+1,n} + K_n(z_{n+1} - H\hat{x}_{n+1,n}) \quad (7)$$

$$P_{n+1,n+1} = \hat{P}_{n+1,n} - K_n S_n K_n{}^T \quad (8)$$

Where $S_n$, and $K_n$ are the innovation covariance and the Kalman gain respectively [5].

With the estimated state variables, equivalences between the kinematic equations of circular motion and the mathematical equations set in the KF structure are utilized, aiming to estimate both the installation parameters and the defined degrees of freedom in each iteration.

Lastly, this geometric information is used to project the accelerometer reading onto a reference base fixed to the ground. These accelerations, having removed the effect of gravitational acceleration ($\{0,0,g\}_{ground}$), are processed using Fast Fourier Transforms and also interpolated and averaged at discrete azimuthal positions to reach the value and evolution of the structure's dynamic response in both, the frequency, and angular domains.

## 3. THE ALGORITHM

### 3.1 Step 1: IMU installation parameters estimation.

Considering the orientation diagram given in Fig 1, the IMU gyroscope rotating with the hub will sense the movement according with the following expressions:

$$\{\overline{\omega}\}_{IMU} = \begin{Bmatrix} \omega_{xImu} \\ \omega_{yImu} \\ \omega_{zImu} \end{Bmatrix}_{IMU} = \begin{Bmatrix} -\dot{\theta}cos(\beta_1)cos(\beta_2) \\ -\dot{\theta}cos(\beta_1)sin(\beta_2) \\ sin(\beta_1)\dot{\theta} \end{Bmatrix}_{IMU} \quad (9)$$

The angular velocity given by the gyroscope can be modelled as a Random Walk variable. This hypothesis, which is consistent with the WT operation, applies to the three components in the IMU reference frame, and allows the KF state transition equation (5) to be expressed as:

$$\hat{\omega}_{n+1,n} = f(\hat{\omega}_{n,n}, u) = \hat{\omega}_{n,n} = \begin{Bmatrix} \hat{\omega}_{xImu\ n,n} \\ \hat{\omega}_{yImu\ n,n} \\ \hat{\omega}_{zImu\ n,n} \end{Bmatrix}_{IMU} \quad (10)$$

Based on this estimation and the kinematic model, equation (9), the installation angles can be estimated:

$$\hat{\beta}_{2,n+1} = \text{atan}\left(\frac{\hat{\omega}_{yImu,n+1,n}}{\hat{\omega}_{xImu,n+1,n}}\right) \quad (11)$$

$$\hat{\beta}_{1,n+1} = -\text{atan}\left(\frac{\hat{\omega}_{zImu,n+1,n}}{\hat{\omega}_{xImu,n+1,n} * cos\hat{\beta}_{2,n+1}}\right) \quad (12)$$

Moreover, the instantaneous phase based on the filtered angular velocity, $\hat{\theta}_{gyro}$ , is calculated:

$$\hat{\theta}_{gyro,n+1} = \|\hat{\omega}_{n+1,n}\|\Delta t + \hat{\theta}_{gyro,n} \quad (13)$$

### 3.2 Step 2: WT azimuth and Tilt estimation.

The measured acceleration and angular velocity are projected in the IMU_Aux1 reference frame using the rotation matrixes defined by $\hat{\beta}_2$ , $\hat{\beta}_1$

$$\begin{Bmatrix}\omega_x\\ \omega_y\\ \omega_z\end{Bmatrix}_{IMU\ Aux1} = \begin{bmatrix} cos\hat{\beta}_1 & 0 & sin\hat{\beta}_1 \\ 0 & 1 & 0 \\ -sin\hat{\beta}_1 & 0 & cos\hat{\beta}_1 \end{bmatrix} \begin{bmatrix} cos\hat{\beta}_2 & -sin\hat{\beta}_2 & 0 \\ sin\hat{\beta}_2 & cos\hat{\beta}_2 & 0 \\ 0 & 0 & 1 \end{bmatrix} \begin{Bmatrix}\omega_{xImu}\\ \omega_{yImu}\\ \omega_{zImu}\end{Bmatrix}_{IMU} \quad (14)$$

$$\begin{Bmatrix}\mathrm{Acc_x}\\ \mathrm{Acc_y}\\ \mathrm{Acc_z}\end{Bmatrix}_{\mathrm{IMU\ Aux1}} = \begin{bmatrix} \cos\hat{\beta}_1 & 0 & \sin\hat{\beta}_1 \\ 0 & 1 & 0 \\ -\sin\hat{\beta}_1 & 0 & \cos\hat{\beta}_1 \end{bmatrix} \begin{bmatrix} \cos\hat{\beta}_2 & -\sin\hat{\beta}_2 & 0 \\ \sin\hat{\beta}_2 & \cos\hat{\beta}_2 & 0 \\ 0 & 0 & 1 \end{bmatrix} \begin{Bmatrix}\mathrm{Acc_{xImu}}\\ \mathrm{Acc_{yImu}}\\ \mathrm{Acc_{zImu}}\end{Bmatrix}_{\mathrm{IMU}} \quad (15)$$

The acceleration components intrinsic to the circular motion of the rotor at the IMU given orientation and installation point, projected in the *IMU_Aux1* reference frame can be formulated as:

$$\widetilde{Acc}_x = R\ddot{\beta}_3 \cos\theta - gsin\beta_3 - 2R\dot{\beta}_3\dot{\theta}sin\theta \quad (16)$$

$$\begin{aligned}\widetilde{Acc}_y = {} & -R\dot{\beta}_3^2 \sin\beta_4 \cos^2\theta - R\,\dot{\beta}_3^2 \cos\beta_4 \sin\theta\cos\theta - R\dot{\theta}^2 \sin\beta_4 \\ & + g\cos\beta_3 \sin\beta_4 \cos\theta - R\ddot{\theta}cos\beta_4 + g\cos\beta_3 \cos\beta_4 \sin\theta\end{aligned} \quad (17)$$

$$\begin{aligned}\widetilde{Acc}_z = {} & -R\dot{\beta}_3^2 \cos\beta_4 \cos^2\theta + R\,\dot{\beta}_3^2 \sin\beta_4 \sin\theta\cos\theta - R\dot{\theta}^2 \cos\beta_4 \\ & + g\cos\beta_3 \cos\beta_4 \cos\theta - R\ddot{\theta}sin\beta_4 + g\cos\beta_3 \sin\beta_4 \sin\theta\end{aligned} \quad (18)$$

The tangential component of the acceleration, $Acc_y$ is modelled as a sinusoidal waveform:

$$\widetilde{Acc}_y = z(t) = \alpha(t)\sin\theta_{gyro}(t) + \beta(t)\cos\theta_{gyro}(t) + v(t) \quad (19)$$

in which $\alpha(t)$ and $\beta(t)$, the state variables, can be estimated using a KF modelling them as autoregressive AR(1). Later, as described in [6] the instantaneous phase given by the gyroscope is corrected with the acceleration phase estimation building an estimator for the actual azimuth, $\hat{\theta}(t)$ as:

$$\hat{\theta}(t) = \hat{\theta}_{gyro}(t) - atan\frac{\hat{\alpha}(t)}{\hat{\beta}(t)} \quad (20)$$

The normal and axial components of the acceleration, $Acc_z$, $Acc_x$ are also modelled as sinusoidal waveforms:

$$\widetilde{Acc}_z = z_N(t) = \alpha_N(t)\sin\hat{\theta}(t) + \beta_N(t)\cos\hat{\theta}(t) + DC_N + v(t) \quad (21)$$

$$\widetilde{Acc}_x = z_A(t) = \alpha_A(t)\sin\hat{\theta}(t) + \beta_A(t)\cos\hat{\theta}(t) + DC_A + v(t) \quad (22)$$

where $\alpha_N(t), \alpha_A(t), \beta_N(t), \beta_A(t), DC_N$ and $DC_A$ can again be estimated using a KF in which they are considered the state variables, with an autoregressive behavior in terms of state transition.

Equations ( 18 ) and ( 16 ) are used in every iteration to estimate the angles $\hat{\beta}_3$ , $\hat{\beta}_4$ :

$$\hat{\beta}_{4\,n+1} = \text{atan}(\frac{\hat{\alpha}_{N\,n+1,n}}{\hat{\beta}_{N\,n+1,n}}) \quad (23)$$

$$\hat{\beta}_{3\,n+1} = \text{asin}(\frac{\widehat{DC}_A}{g}) \quad (24)$$

And finally, it can be constructed the corresponding rotation matrices used to get the acceleration in the ground reference:

$$\{\overline{Acc}\}_{Ground} = \begin{Bmatrix} Acc_{xGround} \\ Acc_{yGround} \\ Acc_{zGround} \end{Bmatrix}_{Ground} \quad (25)$$

$$= \begin{bmatrix} cos\hat{\beta}_3 & 0 & sin\hat{\beta}_3 \\ 0 & 1 & 0 \\ -sin\hat{\beta}_3 & 0 & cos\hat{\beta}_3 \end{bmatrix} \begin{bmatrix} 1 & 0 & 0 \\ 0 & cos\,(\hat{\beta}_4 + \hat{\theta}) & -\sin\,(\hat{\beta}_4 + \hat{\theta}) \\ 0 & \sin\,(\hat{\beta}_4 + \hat{\theta}) & cos\,(\hat{\beta}_4 + \hat{\theta}) \end{bmatrix} \begin{Bmatrix} Acc_{xImu} \\ Acc_{yImu} \\ Acc_{zImu} \end{Bmatrix}_{IMU\_Aux1}$$

### 3.3 Step 3: Accelerometer frequency and angular domain decomposition

Finally, the acceleration measured in the hub, expressed in the ground reference, $\{\overline{Acc}\}_{Ground}$, can be subjected to detailed analysis. Each component is processed using Fast Fourier Transforms (FFT), a mathematical algorithm that converts time-domain data into the frequency domain. This transformation offers a clear perspective on the frequency components within each component. Importantly, the FFT can be paired with harmonic elimination techniques, as detailed in [7], to remove components associated with rotational harmonics. This meticulous approach ensures that the resulting spectrum primarily represents the response aligned with the modal frequencies of the WT.

For a more comprehensive understanding of the structure's dynamic behavior, the data should also undergo interpolation or bin averaging, guided by the reference provided by $\hat{\theta}$ and using real-time compatible techniques such as Catmull Rom splines [8]. When averaged at specific azimuthal positions, the results capture the fundamental essence of the dynamic response at these operating points.

By examining this processed data, we can adeptly measure both the intensity and progression of the structure's response across two crucial domains: frequency and angular.

## 4. VALIDATION PROCESS. DESCRIPTION AND RESULTS.

To validate the algorithm presented in the previous sections, the OpenFAST simulation tool has been used. This virtual framework enables the generation of synthetic signals that mimic acceleration and gyroscope measurements at specific locations on the wind turbine. OpenFAST is an open-source software designed for conducting integrated nonlinear simulations of WT in the time domain, encompassing aero, hydro, servo, and structural aspects. This software was developed by the National Renewable Energy Laboratory (NREL) and holds certification for the design of both onshore and offshore wind turbines. In this study, a 5 MW NREL onshore reference wind turbine, featuring a 3-bladed, 126 m diameter wind rotor mounted on an 87.6 m

tall tower, serves as the benchmark and has found widespread application in numerous research investigations [9].

For the validation of the previously described methodology and algorithm, OpenFAST enables to model and locate an IMU at different locations on the rotor and at different radial distances from the axis of rotation. Different IMU installation angles have been modelled. Other configurable parameters include wind type, wind speed, and hub tilt angle. These scenarios have been used to validate the algorithm in an environment very close to what the IMU will encounter in practice.

Finally, leveraging OpenFAST's ability to simulate acceleration measurements in different parts of the wind turbine, we compared the results from the hub location using our proposed real-time algorithm and the standalone IMU to those from traditional CMS. Traditional CMS systems, which measure accelerations at nacelle locations, often require higher true resolution sensors and additional measurements or connections to the turbine's operating system to contextualize the data.

The algorithm has been tested against various OpenFAST configurations, however, due to space constraints, only the results obtained in a specific case are going to be presented. In this scenario, a deterministic wind speed of 12 m/s was used, as shown if Fig 2, and the IMU was placed at a radius of R=0.5m from the axis of rotation. The IMU was placed assuming the following initial values $\beta_1 = 5º$, $\beta_2 = -4º$, $\beta_3 = 5º$ and $\beta_4 = 0º$.

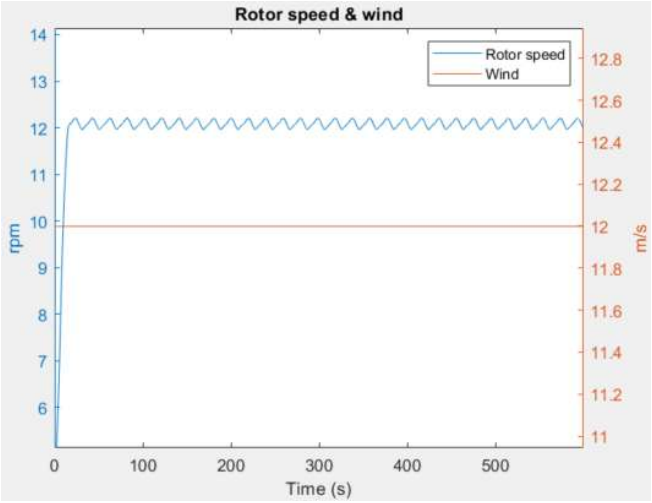


Fig 2. OpenFAST simulated load case.

Next, the estimation errors for various parameters and geometric variables are presented in comparison to the virtual results from OpenFAST for the described operational case.

### 4.1 IMU Installation angles $\beta_1, \beta_2$

As described in the algorithm section, the first step is to estimate the installation angles that occur when the IMU is placed on the rotor $\beta_1, \beta_2$, which for the OpenFAST simulation have been set to 5º and -4º respectively. The estimation performed is illustrated in Fig 3.

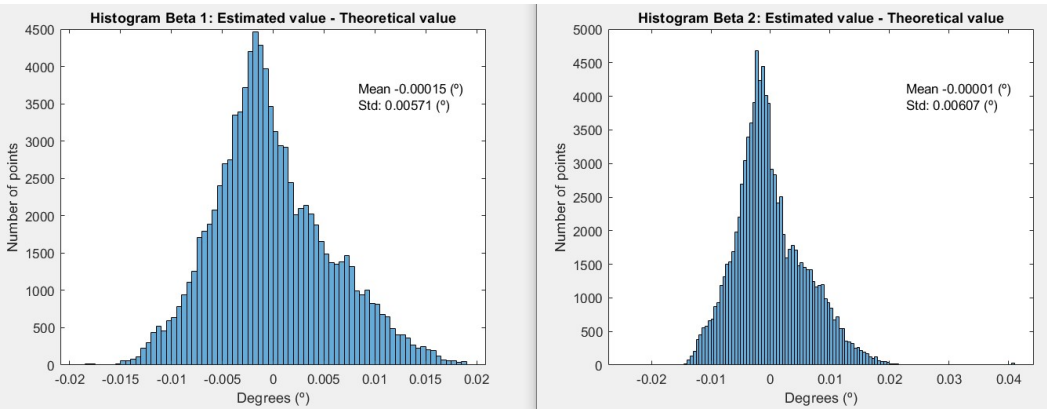


Fig 3. Histogram of estimation error value of IMU misalignment angles in its placement, $\hat{\beta}_1$ , $\hat{\beta}_2$

As depicted in the histograms, the estimation bias and standard deviation relative to the initial installation parameters are negligible.

### 4.2 Azimuthal Coordinate $\theta, \beta_4$ and Hub Tilt $\beta_3$

Estimation evaluations corresponding with the azimuth, $\hat{\theta}, \hat{\beta}_4$ and hub tilt, $\hat{\beta}_3$ , with respect to an initial value $\beta_3 = 5º, \beta_4 = 0º$ and unknown azimuthal position are analyzed in Fig 4.

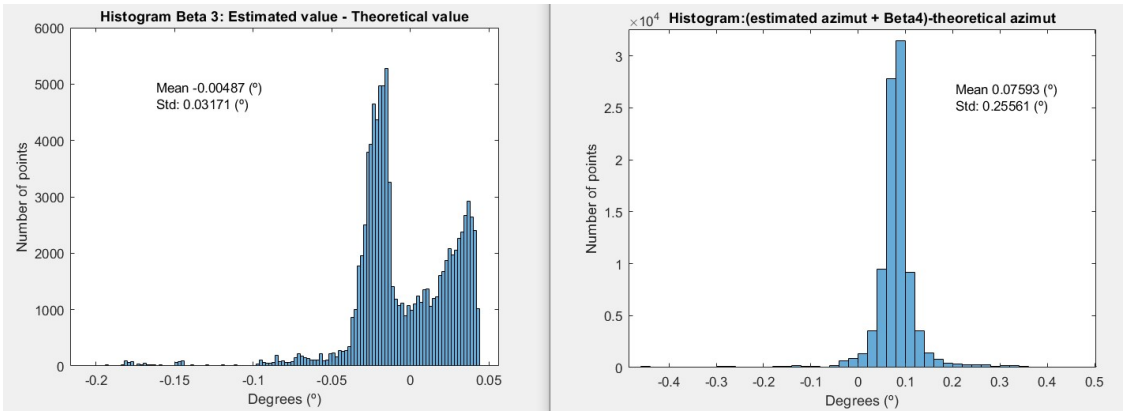


Fig 4. Histogram of the difference between the estimated $\hat{\theta} + \hat{\beta}_4$ , $\hat{\beta}_3$ and OpenFAST simulation

Again, as shown in the histograms, relatively small errors in terms estimation bias and standard deviation are given for the case of the turbine considered operation degree of freedom.

### 4.3 Acceleration Decomposition

As it has been explained, once the geometric parameters have been estimated, the rotation matrices are constructed from these parameters. These matrices are used to project the acceleration given by the IMU placed on the reference base fixed to the ground. Finally, the projected acceleration is then compared with the acceleration generated by OpenFAST for a

point on the nacelle. Both accelerations are expressed in the same reference frame. This can be seen in Fig 5.

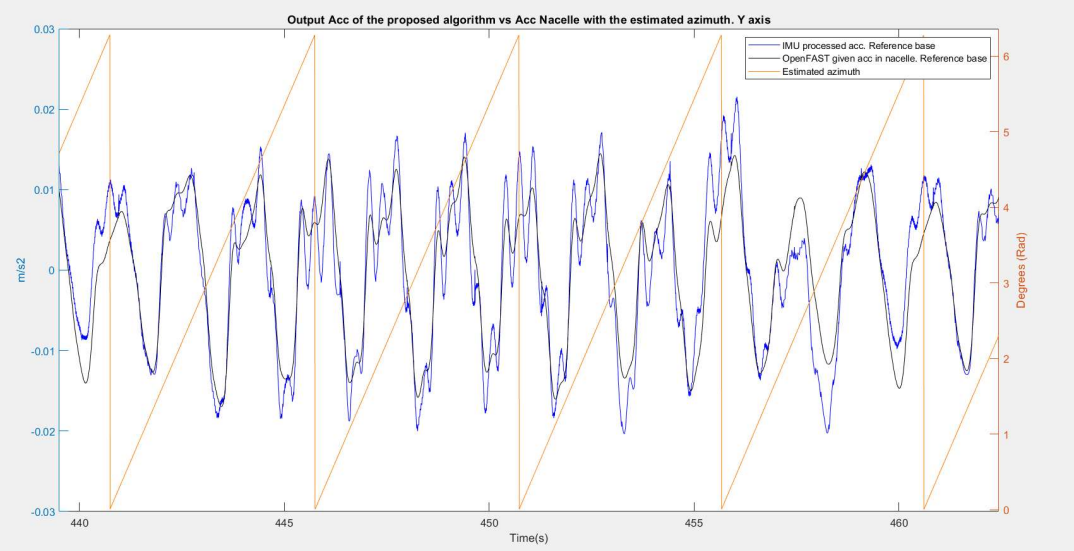


Fig 5. Comparison in time domain of the acceleration given by OpenFAST in X direction for a nacelle location in a ground fixed reference with the acceleration given in the same direction for a Hub location processed with the described algorithm.

The same comparison is made in the frequency domain in Fig 6

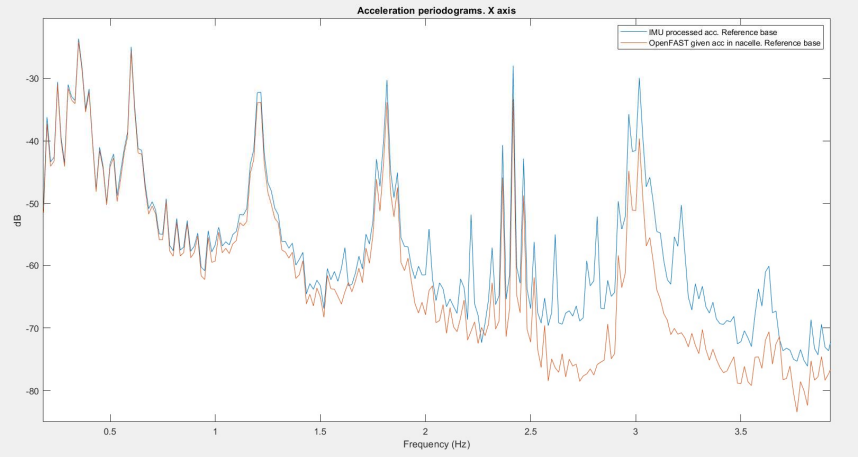


Fig 6. Comparison in frequency domain of the acceleration given by OpenFAST in X direction for a nacelle location in a ground fixed reference with the acceleration given in the same direction for a Hub location processed with the described algorithm.

It is evident from the two graph the closeness between the accelerations obtained in the nacelle with those resulting from the applications of the algorithm in both time and frequency

domains. Only behavior beyond, say, 2 Hz diverges, which is less relevant to assess tower dynamics, but it can reveal sensitivity to other components (hub and blades).

Finally, the acceleration given at the Hub location $\{\overline{Acc}\}_{Ground}$is examined in conjunction with the estimated azimuth, $\hat{\theta}$. The 600-second time series for each $\{\overline{Acc}\}_{Ground}$ components are categorized into bins of 5º corresponding to the azimuth. Both the mean value and standard deviation for each bin are computed. Fig 7 illustrates the mean values (of each rotation along 600s) of $Acc_{yGround}$ overlaid with 1-sigma intervals.

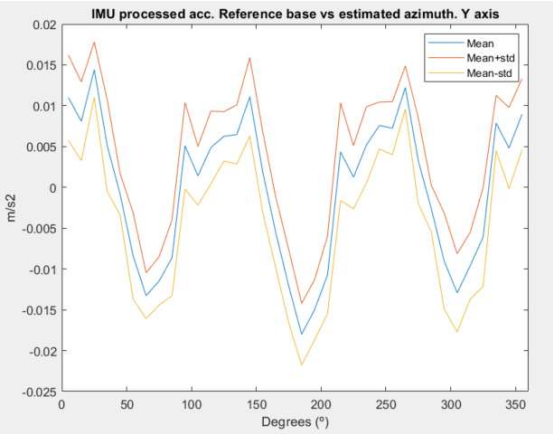


Fig 7. $Acc_{yGround}$.vs $\hat{\theta}$.

Notably, the contributions of the three blades to the dynamic response are distinctly isolated. This enables trend analysis, which can be employed to pinpoint rotational defects such as mass imbalances or aerodynamic irregularities.

## 5. CONCLUSIONS

In this paper we have proposed an IMU placed on the main shaft of a WT, as an alternative to conventional nacelle or tower fixed sensors to assess its structural health. A combination of algorithms is proposed to calculate the precise rotor azimuth and estimate the actual orientation of the IMU and thus recalculate its measured accelerations to a ground reference.

The study carried out successfully validated an innovative algorithm in a simulated environment closely mirroring real-world conditions, using OpenFAST. Notably, the algorithm's results aligned well with accelerations measured at the turbine's nacelle, solidifying its credibility. Also, the combinations of the accelerations with the precise knowledge of the rotor azimuth, has been shown as a potential powerful tool to identify the source of possible failures.

## 6. ACKNOWLEDGEMENTS

This paper has been supported by the Spanish Research Agency, and the EU/PTR Next Generation Funds under grants PID2019-107258RB-C32, TED2021-131052B-C21, and PID2022-138491OB-C32. I. Vilella is supported by a grant for “Industrial Doctorates 2021”

from the Government of Navarre.

## 7. REFERENCES

[1] M. L. Wymore, J. E. Van Dam, H. Ceylan, and D. Qiao, "A survey of health monitoring systems for wind turbines," *Renewable and Sustainable Energy Reviews*, vol. 52. Elsevier Ltd, pp. 976–990, Aug. 22, 2015. doi: 10.1016/j.rser.2015.07.110.

[2] A. P. Daga and L. Garibaldi, "Machine vibration monitoring for diagnostics through hypothesis testing," *Information (Switzerland)*, vol. 10, no. 6, Jun. 2019, doi: 10.3390/info10060204.

[3] A. Plaza, J. Ros, G. Gainza, and J. D. Fuentes, "Triaxial accelerometer based azimuth estimator for horizontal axis wind turbines," *Journal of Wind Engineering and Industrial Aerodynamics*, vol. 240, Sep. 2023, doi: 10.1016/j.jweia.2023.105463.

[4] L. F. Villa, A. Reñones, J. R. Perán, and L. J. De Miguel, "Angular resampling for vibration analysis in wind turbines under non-linear speed fluctuation," *Mechanical Systems and Signal Processing*, vol. 25, no. 6. pp. 2157–2168, Aug. 2011. doi: 10.1016/j.ymssp.2011.01.022.

[5] M. S. Grewal and A. P. Andrews, *Kalman Filtering: Theory and Practice Using MATLAB®: Third Edition*. John Wiley and Sons, 2008. doi: 10.1002/9780470377819.

[6] M. Zivanovic, I. Vilella, X. Iriarte, A. Plaza, G. Gainza, and A. Carlosena, "Main Shaft Instantaneous Azimuth Estimation for Wind Turbines," *Mech Syst Signal Process*.

[7] M. Zivanovic, A. Plaza, X. Iriarte, and A. Carlosena, "Instantaneous amplitude and phase signal modeling for harmonic removal in wind turbines," *Mech Syst Signal Process*, vol. 189, Apr. 2023, doi: 10.1016/j.ymssp.2023.110095.

[8] E. Bechhoefer and M. Kingsley, "A Review of Time Synchronous Average Algorithms," in *Conference of the Prognostics and Health Management Society*, 2009.

[9] K. A. Stol, H.-G. Moll, G. Bir, and H. Namik, "A Comparison of Multi-Blade Coordinate Transformation and Direct Periodic Techniques for Wind Turbine Control Design," in *47th AIAA Aerospace Sciences Meeting Including The New Horizons Forum and Aerospace Exposition*, Orlando, Jan. 2009.